**Title**
193 nm Photodissociation of Acetylene



**Journal**
Journal of chemical physics, 94(12)

**Authors**
Balko, B.A.
Zhang, J.
Lee, Yuan T.

**Publication Date**
1991

LBL-30184
Preprint

# Lawrence Berkeley Laboratory
UNIVERSITY OF CALIFORNIA

## Materials & Chemical Sciences Division

Submitted to Journal of Chemical Physics

**193 nm Photodissociation of Acetylene**

B.A. Balko, J. Zhang, and Y.T. Lee

January 1991



Prepared for the U.S. Department of Energy under Contract Number DE-AC03-76SF00098

## DISCLAIMER

LBL-30184

# 193 NM PHOTODISSOCIATION OF ACETYLENE

B. A. Balko, J. Zhang, and Yuan T. Lee

Department of Chemistry
University of California

and

Chemical Sciences Division
Lawrence Berkeley Laboratory
Berkeley, CA 94720 USA

January 1991

This work was supported by the Director, Office of Energy Research, Office of Basic Energy Sciences, Chemical Sciences Division, of the U.S. Department of Energy under Contract No. DE-AC03-76SF00098.

# 193 nm Photodissociation of Acetylene

B.A. Balko, J. Zhang, and Y.T. Lee
Department of Chemistry, University of California at Berkeley and
Chemical Sciences Division, Lawrence Berkeley Laboratory
Berkeley, CA 94720

**ABSTRACT**

The product translational energy spectrum of acetylene photodissociation at 193 nm was obtained via mass spectrometric detection of the H atom fragments. Comparison of the H atom time-of-flight spectrum with the known $C_2H$ spectrum shows $D_0(HCC-H) = 131.5 \pm .5$ kcal/mole, in agreement with our group's previous measurements and the latest experimental and theoretical studies. Our spectra have enough resolution for us to confirm and suggest $C_2H$ spectrum assignments; we agree with Kanamori and Hirota's X(0 7 0) assignment and have identified higher C-H bending peaks that could correspond to some of Jacox and Olson's unidentified $C_2H$ lines. The results also offer new insight to the primary and secondary photodissociation processes.

## 1. INTRODUCTION

The 193 nm photodissociation of acetylene provides a means to measure some fundamental properties of the $C_2H_2$ parent and the photoproduct, $C_2H$. Although acetylene and the ethynyl radical are important in combustion processes [1] (acetylene has, in fact, been called the "key intermediate" in soot formation [2]), many of their properties are not well known. For example, the

HCC-H bond energy is controversial and the strong coupling between the $C_2H(A^2\Pi)$ and $C_2H(X^2\Sigma_g^+)$ electronic states makes determining vibrational and electronic transitions difficult.

The time-of-flight (TOF) technique used in this study is a direct measure of the product translational energy. As the energy conservation equation for a photodecomposition process shows, this allows us to obtain a value for $D_0$(HCC-H) and determine the internal energy distribution in $C_2H$:

$$h\nu + E_{Int,C_2H_2} - D_o(HCC\text{-}H) + E_{Int,C_2H+H} + E_{Trans,C_2H+H}.$$

If one assumes that most of the parent molecules will be in the ground state (usually not a bad assumption for molecular beam studies) and that some of the products will be formed internally cold, the fast edge of the TOF spectrum, where the product internal energy should be zero, can be used to derive the bond energy. Since the $E_{Int,product} = 0$ assumption is generally considered the weakest, this value will be an upper limit. The equation also shows that the TOF spectrum mirrors the internal energy distribution of the products [3]. For the case of acetylene, since only $H(^2S)$ can form (the next H electronic state is 235 kcal/mole higher), the TOF spectrum represents the internal energy distribution of the elusive $C_2H$.

Five years ago, our group measured the HCC-H bond energy from the translational energy spectrum of the $C_2H$ fragments after the 193 nm photodissociation of $C_2H_2$ [4]. This value was in agreement with others determined using different techniques [5,6]. In 1989, however, two groups reported numbers which were

significantly lower [7,8]. These measurements brought the acetylene C-H bond energy into question again and initiated a flurry of experimental [9,10,11] and theoretical studies [12,13,14,15] (see Table I). As a check on our group's original measurement, we decided to restudy the 193 nm $C_2H_2$ photodissociation, but this time record the TOF spectrum of the resulting H atoms. Since one of the experiments that recorded the lower bond energy involved H atom translational energy measurements [7], our new study can give some insight to the cause of the difference. With H atom detection, we also have an easy way to calibrate the experimental set-up, reducing the possibility of systematic errors; under the same experimental conditions, we can look at the photodissociation of DI and HI, which have well determined bond energies and a known $I(^2P_{1/2}) \leftarrow I(^2P_{3/2})$ energy spacing.

The high resolution 193 nm photodissociation of $C_2H_2$ is also an excellent means of learning about the vibrational and electronic energy states of the resulting $C_2H$ fragment since these states should not be significantly smeared out by rotational excitation. The parent $C_2H_2$ should initially be fairly cold due to cooling in the molecular beam expansion. Rotational excitation of the $C_2H$ fragment, then, will be equal to the orbital angular momentum of the H atom leaving the $C_2H$. Owing to the light mass of the H atom and a relatively small exit impact parameter, this contribution should be small, especially at lower translational energies. In our study of the $C_2H_2$ 193 nm

photodissociation, we hoped that the high resolution TOF spectra of H atoms along with the improved detector calibration would provide more accurate values for the product internal energy states than obtained previously in our group. We also have the advantage of new studies on the $C_2H$ vibrational and electronic states that have appeared since Wodtke and Lee's paper that will aid in our interpretation of the product translational energy spectrum.

In addition to helping clear up some questions about the acetylene and ethynyl molecules, the 193 nm photodissociation studies are useful for understanding the process itself and can reveal information about the potential energy surfaces of the states involved [16]. The $C_2H_2$ dissociation is an especially interesting case because of the confusion of states in the $C_2H$ system [17]. The expected (and observed) coupling between the $C_2H$ A and X electronic states means that the Born-Oppenheimer approximation, a standard assumption in many photodissociation models, is not appropriate [18].

Much is already known about the 193 nm photodissociation of acetylene. At 193 nm, acetylene absorbs to $\nu_3 = 10$ (the C-H bending vibration) of the $^1A_u$ excited state [19]. The acetylene absorption has been studied extensively in the range 1970-2500 Å and this work established that the $^1A_u$ excited state has a trans-bent configuration ($C_{2h}$ symmetry) [20,21]. Figure 1 [9,22,23,24] shows the products that are thermodynamically possible. At low laser intensities, $< 10^{26}$ photons/cm$^2$s, the primary process Wodtke

and Lee observed during the 20 nsec photolysis pulse is:

$$C_2H_2 \rightarrow C_2H + H \qquad (I).$$

It was not possible for them to determine unambiguously whether $C_2H$ formed in just the X state or both the X and A states [4]. This question was cleared up in Fletcher and Leone's FTIR study of the $C_2H$ products from the 193 nm photodissociation of $C_2H_2$ where they detected $C_2H$ in both electronic states [25]. As discussed by Wodtke and Lee, because of the large changes in the equilibrium C-C bond lengths and C-C-H bond angles that occur during the dissociation process, $C_2H_2(X) \rightarrow C_2H_2(^1A_u) \rightarrow C_2H(A \text{ or } X)$, one expects the $C_2H(A,X)$ C-C stretch and C-H bend to be excited [4]. Thus, it is not surprising that in Fletcher and Leone's study, X(0 5 1), X(1 1 0), and A(0 1 0) were detected [25]. No evidence has been found for the only other one photon channel thermodynamically allowed:

$$C_2H_2 \rightarrow C_2 + H_2 \qquad (II).$$

Wodtke and Lee did not detect $C_2$ from this channel but in their "worst case scenario" this channel could be ≤15% of I and still not be observed because of the complication caused by the $C_2$ formed from the secondary photodissociation of $C_2H$[4].

At higher laser intensities, more channels open up. McDonald's early emission studies on the multiphoton photodissociation of $C_2H_2$ identified several two and three photon processes. Most (≥ 90%) of the measured emission intensity was from the $C_2(A^1\Pi_u \rightarrow X^1\Sigma_g^+)$ transition in which states as high as $A^1\Pi_u$ v = 5 were observed. Their observations were consistent with a

two photon process that proceeds via sequential elimination of two H atoms:

$$C_2H_2 \rightarrow C_2H + H$$

$$C_2H \rightarrow C_2 + H$$

Emission from $C_2(d^3\Pi_g \rightarrow a^3\Pi_u)$ was also detected but this was only a minor channel (~1% of the $A^1\Pi_u$); based on lifetime measurements and the power dependence, they concluded that three photons were absorbed but could not determine the mechanism. Fluorescence from $CH(A^2\Delta \rightarrow X^2\Pi)$ was recorded; this channel was also minor (< 1% of $A^1\Pi_u$). The production of $CH(A_2\Delta)$ appeared to proceed via two photon excitation of $C_2H_2$ -- the $C_2H$ intermediate was not involved. Finally, emission from $C_2(C^1\Pi_g \rightarrow A^1\Pi_u)$ was reported but the signal was not intense enough (< 1% of $A^1\Pi_u$) to derive any mechanistic information [26]. Wodtke and Lee also saw evidence of multiphoton processes in their studies. The $C_2(A^1\Pi_u, {}^3\Pi_u, X^1\Sigma_g^+)$ that they detected formed via two sequential one photon absorption steps: $C_2H_2 \rightarrow C_2H \rightarrow C_2$ [4]. Recently, several more electronically excited $C_2$ states have been detected from the sequential 193 nm photolysis of $C_2H_2$. Using LIF methods, Urdahl, Bao, and Jackson reported the formation of $C_2(a^3\Pi_u, d^3\Pi_g, A^1\Pi_u,$ and $C^1\Pi_g)$ with the following relative populations: $a^3\Pi_u > d^3\Pi_g$; $A^1\Pi_u >> C^1\Pi_g$; $a^3\Pi_u \approx A^1\Pi_u$ [27]. Goodwin and Cool detected the presence of $C_2(B^1\Delta_g)$ up to v=2 and $C_2(b^3\Sigma_g^-)$ in the two step photolysis of $C_2H_2$ [28]. Recently, Bao, Urdahl, and Jackson have found evidence of $C_2(B'^1\Sigma_g^+)$ from a two photon sequential process [29].

The formation of some of these higher excited states for $C_2$

is only energetically possible if the intermediate $C_2H$ is internally excited. In fact, by studying the change in shape of the $C_2H$ TOF spectra with laser power, Wodtke and Lee showed that the $C_2H$ absorption cross section was larger for more highly excited $C_2H$ molecules [4]. From what is known about the $C_2H$ radical excited electronic states, this is not surprising. The lowest lying electronic states for which a transition from the $^2\Sigma^+$ ground state is allowed are $^2\Sigma^+$ and $^2\Pi$. These states have vertical excitation energies of 7.32 eV and 8.11 eV, respectively. The transition energy, however, drops to the 193 nm range if one assumes that the upper state is bent in its equilibrium configuration and that the initial state's C-C bond length is greater than the equilibrium value and/or the C-C-H angle is not 180° [17,30,31].

## 2. EXPERIMENT

In reinvestigating the 193 nm photodissociation of acetylene, the same method--photofragmentation translational spectroscopy-- is used but the studies are done with a high resolution fixed source/rotating detector molecular beam apparatus [32]. This machine was recently modified to allow the use of a pulsed photolytic beam source (see Figure 2) [33]. Briefly, a homemade piezo-electric pulsed valve is mounted so it fires into a small chamber pumped by a 4" DP and a liquid nitrogen cooled cryopanel. To permit higher resolution studies, a skimmer can be inserted between the pulsed valve nozzle and

laser interaction region to reduce the angular spread of the acetylene beam. The focused output of an ArF Lambda Physik 202 MSC ILC excimer laser enters this chamber, crossing the molecular beam perpendicularly. This configuration is especially suited to photodissociation experiments because the photofragments will travel a long distance (39.0 cm) before being detected which allows us to obtain well-resolved TOF spectra.

The use of this machine for photodissociation studies means the experiment must be done differently than Wodtke and Lee's. The source construction necessitates detection perpendicular to the parent beam direction. As the kinematic (Newton) diagram illustrates (see Figure 3), experimentally, this means that the slowest product velocity we can detect will be the one where the velocity in the center-of-mass (COM) reference frame is equal to the parent beam velocity. To obtain as complete a product translational energy distribution as possible, one must detect the faster product which, based on the conservation of linear momentum, will be the lighter one. Thus, in our studies of $C_2H_2$ photodissociation, we look at the H atom. Most (~75%) of this product appears with a COM velocity between 113.5 and 49.1 x $10^4$ cm/s (17-8 times the parent velocity).

This experimental scheme has several advantages over that of Wodtke and Lee. First, since the product angular distribution is isotropic [4], by looking at the fast H atoms, we are able to see the entire product energy distribution at the one laboratory angle; there is no need to piece together data acquired at

several different angles. Second, as the Newton diagrams show, detection of the fast product also means that improved TOF resolution is possible since the H atom velocity will not be significantly perturbed by the distribution of parent beam velocities and angles. This allows us to use a beam which is less defined but with a much higher intensity. Finally, since we are detecting product 90° from the parent beam, we have less background caused by the dissociative ionization of the parent molecules which becomes a problem at lab angles close to the beam like Wodtke and Lee were forced to go to (6° to 28°).

Of course, our technique has its own disadvantages. The very low energy tail (< 3 kcal/mole) of the product translational energy spectrum cannot be well determined. The problem is the slow temporal background which is mainly due to $H^+$ that result from fragmentation of the thermalized parent pulsed beam arriving at the detector. To a large extent, the interference of this background can be reduced by recording a laser-off spectrum and subtracting it from the laser-on (see Figure 4). Another difficulty is that with the detector 90° from the beam we cannot detect the $C_2H$ fragment so we have to be more aware of interference from multiphoton events than Wodtke and Lee did; the H atoms we see can either come from the primary process, $C_2H_2 \rightarrow C_2H + H$, or the secondary, $C_2H \rightarrow C_2 + H$. To get a true picture of the primary process, we need to go to very low laser power where the signal becomes poor. Finally, fast H atoms are more difficult to detect. At the low quadrupole RF voltages necessary

for mass selection of the H atoms, we have a problem with laser RF pick-up which causes a time dependent variation in the transmission of the quadrupole mass filter. For long, low-signal runs at small masses at times $\leq 50\mu$sec, we find large fluctuations in the background as long as the laser is running (it does not have to enter the chamber). Unfortunately, these modulations are right at the rising edge of the photofragmentation signal -- where we need to look to determine the bond energy. Our initial solution was to record backgrounds (laser flagged but running) of this modulation and then subtract this signal away (see Figure 5). Later, we found that putting an RF power line filter (Corcom EMI 10VR7) on the mass spectrometer controller AC input line would essentially eliminate this noise. We compared the corrected TOF spectra with that taken using the filter and saw no difference. Another difficulty inherent in H atom detection is that our detector is less sensitive to H atoms. This is both because of their velocity, which limits their time in the electron bombardment ionizer, and because the ionization cross sections for H atoms are smaller than for molecules such as $C_2H$ [34].

The data discussed here was collected under several different conditions. In all the work, however, the pulsed parent beam was formed by passing $C_2H_2$ gas (Matheson) through a dry ice/acetone trap and into the piezo-electric pulsed valve (1 mm nozzle). In the low resolution experiments, the laser crossed the molecular beam approximately 3 mm from the nozzle.

The acetylene stagnation pressure typically used under these conditions was 30-50 torr. High resolution experiments were also done; instead of photolyzing in the free jet, the acetylene, at a stagnation pressure of 75 torr, first passed through a skimmer (nozzle/laser distance = 2.3 cm). There was more than twice as much m/e = 1 signal observed when in low-resolution mode; unfortunately, there was also more collisional broadening which smears out the $C_2H$ vibrational structure in the TOF spectra. To reduce the m/e = 1 background, for most of the experiments, the detector opening was chopped with a 2-slot wheel spinning at 25 hz. This left the detector open for > 400 $\mu$sec. To ensure that we were not cutting out any signal, the same measurements were taken without the wheel. The laser power was also varied in the experiments so we could learn about secondary dissociation. Typically, the laser was focused to a 3 x 5 mm spot at the interaction region using a 30 cm spherical Suprasil lens. The range of pulse energies studied was about 20 mj/pulse to 237 mj/pulse (which correspond to $7 \times 10^{24}$ and $8 \times 10^{25}$ photons/cm$^2$sec for the 20 nsec pulse); these values are "before lens". A new, clean lens could typically transmit ~90% of the laser power; after a set of experiments, the lens' transmission would drop to ~70% as a result of photolysis by-product buildup. Because this means the laser power at the interaction region will vary over time, the laser powers given are what is measured before the lens. Most of the data was collected at 125 - 150 mj/pulse at 50 hz. A mixture of HI and DI synthesized in our lab

[33] was run under the same conditions to allow us to calibrate the TOF measurements.

Once the TOF spectra were obtained, the raw data had to be corrected for the pulsed valve temporal background and RF pickup. Scans without laser irradiation were taken throughout the run which could be fit with a polynomial and then subtracted from the photodissociation signal (see Figure 4). The RF pickup correction was discussed previously. The final step before any quantitative information could be derived from the spectra was to calibrate the detector. We used a forward convolution data analysis program [35] to fit the HI and DI TOF spectra. An input translational product energy distribution $P(E_T)$ was generated using the photon energy along with the known bond energies and iodine excitation energies and assuming some initial parent rotational distribution. The program then averaged this over the experimental factors (parent beam velocity, beam spread, detector viewing angle, and laboratory angle); with fine adjustments of the detector parameters (ion flight time, effective length of ionizer, and neutral molecule flight length), good fits to these TOF spectra were obtained. The best values of these detector parameters were then used in fitting the H atom spectra from the $C_2H_2$ photodissociation. In this final analysis, one would guess an input $P(E_T)$ which would then be convoluted over the experimental parameters to obtain the expected TOF; the input $P(E_T)$ was changed until the calculated TOF agreed with the experimental.

## 3. RESULTS

### a. Calibration

Figure 6 shows the H and D atom spectra from the photodissociation of a skimmed beam of HI and DI using the same conditions as the $C_2H_2$ experiments. The solid line is the best fit TOF spectra assuming a rotational temperature of 100K. It should be noted that the fits are not sensitive to the rotational temperature; the peak width is mainly due to the ionizer length. These TOF spectra show the broadening that results from H atoms undergoing collisions in the photolysis region; at the slow edge of the fast peak the fit does not match the observed spectra as well. The differences between spectra with and without the skimmer should also be noted. The skimmer spectrum is narrower; without the skimmer to help define the beam, the photolysis region is larger so there is more spread in the no-skimmer H atom flight length.

### b. Skimmed Beam/High Resolution

As discussed previously, one of the problems in determining the HCC-H bond dissociation energy with our H atom TOF technique is the possibility of contamination from multiphoton and/or sequential dissociation events which can produce faster H atoms than from process I. To get a pure one photon spectrum, we went to very low laser power (~35 mj/pulse) where there were no obvious signs of secondary dissociation and counted for 5.6 hours. The spectrum obtained from the skimmed beam is shown in Figure 7a; because of the poor signal to noise ratio (S/N),

this was only used to obtain the rising (fast) edge of the $P(E_T)$ which was then incorporated in all other fitting. The spectrum shows a good deal of RF-pickup noise at the fast edge even though the data was collected with our RF filter installed; this is because the signal is so poor and we must count for so long that any slight effect the RF modulation may have on the quadrupole mass spectrometer transmission can be observed; the filter apparently does not remove everything. Unfortunately, after the long signal accumulation, we discovered that the background RF noise scans we took no longer match the pickup signal so the spectrum is just displayed as is.

To get enough S/N to be able to say something about the vibrational and electronic states of the $C_2H$ radical, we had to use higher laser powers (~100-150 mj) with the skimmed beam. Figure 7b shows the spectrum after all our runs had been added (21 hours) and all background/RF noise corrections made. The solid line is the TOF calculated using the $P(E_T)$ in Figure 8a. An attempt was made to fit the secondary dissociation products which is discussed later.

Comparing the high resolution $P(E_T)$ we obtained with that of Wodtke and Lee shows good general agreement (see Figure 8b). Our vibrational/electronic resolution, however, seems higher. Most notably, Wodtke's peak 2 (we are employing the same numbering scheme) appears in our $P(E_T)$ as two separate peaks; our TOF spectra is very sensitive to this structure whereas Wodtke and Lee reported that adding such peaks would have little effect on

the calculated TOF spectrum [4]. The other area of difference is the low translational energy section of the $P(E_T)$; we seem to see much more than Wodtke and Lee. One explanation is that highly internally excited $C_2H$ fragments more easily in the detector than ground state $C_2H$; at low translational energies, then, one might expect to see less $C_2H$ (and more $C_2$). Because of the way our experiment is set-up we should not have much $C_2H$ reaching the detector that could subsequently fragment during the ionization to produce more $H^+$ ions so our TOF would not be affected by this differential fragmentation. The other possibility is that our results have some slow H atom laser correlated signal -- perhaps from some laser produced H atoms that, after collisions inside the photolysis chamber, eventually make their way to the detector. The latter explanation is supported by high and low $C_2H_2$ pressure spectra taken with no skimmer. The higher pressure scans have relatively more slow H atoms. At higher pressures, fast H formed could undergo more collisions before exiting which would slow them down resulting in a relative increase in the low $P(E_T)$ H atoms.

The comparison between our high resolution spectra and that of Wodtke and Lee suggests that we too are seeing the effect of unrelaxed $C_2H_2$ bending vibrations. By heating the parent nozzle to 530K, Wodtke and Lee showed that the higher translational energy section of the $P(E_T)$, from ~16 to 18 kcal/mole, was due to photodissociation of $C_2H_2$ that had some initial vibrational excitation, presumably in the two doubly degenerate bends (611

and 729 $cm^{-1}$) [4].

**c. No-Skimmer/Low Resolution**

When photolyzing in the free jet, a good deal of product vibration/electronic state resolution is lost so these spectra cannot be used to derive the internal energy distribution of the primary products. The S/N ratio, however, is much higher making it easier to do laser power studies. Since it is usually difficult to learn many details of the product internal energy distribution in secondary dissociation events because of the wide range of velocities and internal energies of the "initial" reactants [35], we felt that we could use these no-skimmer studies to try to understand the important features of the secondary dissociation process. Figure 9 shows three low resolution H atom TOF spectra taken at different laser powers (~60, 105, and 235 mj/pulse).

In the fitting of these spectra, it is assumed that all the H atoms are either from the primary process, $C_2H_2 \rightarrow C_2H + H$, or from the secondary process, $C_2H \rightarrow C_2 + H$ (sequential photodissociation). Based on the observations of McDonald et. al. [26] this is reasonable since the CH production channel seems to account for < 1% of the secondary signal. There is much uncertainty in fitting the secondary event. One cannot assume that all the $C_2H$ formed has the same probability of undergoing secondary dissociation--more highly internally excited products seem to absorb a photon much more readily [4]. The forward convolution fitting program used allows one to select which

energy $C_2H$ will undergo further fragmentation. The differences between the high and low power TOF spectra indicate that $C_2H$ fragments formed with $E_T \geq 10$ kcal/mole would not undergo further dissociation. There is enough uncertainty, however, in the comparison that this is only an upper bound. We started fitting the secondary products by assuming that only the primary products with $E_T \leq 10$ kcal/mole would be able to dissociate ($E_{T,thres} = 10$ kcal/mole). It was very difficult to fit the high power TOF -- specifically, we could not simulate the "dip" on the rising edge. Using $E_{T,thres} = 7$ kcal/mole was found to be much more successful. We tried lowering $E_{T,thres}$ still further to 5 kcal/mole and still got a fairly good high power fit. $E_{T,thres} = 7$ kcal/mole seemed to give the best fit to the TOF spectra at all powers. Our results, however, do not unambiguously prove that this is the true $E_{T,thres}$; the value could be lower but not significantly (~ 2 kcal/mole) higher. Also, the secondary dissociation probability might have a gradual dependence on the primary product internal energy rather than the step function we are assuming. The secondary $P(E_T)$ that best fit the spectra are bimodal (see Figure 10); this is true no matter what $E_{T,thres}$ was used. The two peaks for the products, $C_2$ + H, have translational energies of ~6 kcal/mole and ~18-19 kcal/mole.

Since the low resolution set-up gives much better S/N, we looked at m/e = 2 to see if there was any evidence for process II. We could see no sign of any $H_2$ product which we would expect to appear at $\geq 100$ $\mu$sec.

## 4. DISCUSSION

### a. Primary Dissociation

As discussed, the HCC-H bond dissociation energy can be determined from the rising edge of the TOF spectrum as long as some ground state product forms. Is this assumption reasonable for this system? While it is expected that high vibrational states of $C_2H$ will form, there is nothing that prohibits the ground state from forming. The $P(E_T)$ for the $C_2H_2$ dissociation peaks away from 0 which is one indication that it is a repulsive process (there is some exit barrier). For this type of half reaction, the energy partitioning tends to be non-statistical in that the fraction of energy going into translation is higher [36]. The repulsive nature of the dissociation would, thus, favor less vibrational excitation. Another reason we would expect to find some ground state $C_2H$ is that the recoiling H atom, due to its small mass, cannot readily excite the $C_2H$ fragment. During the fragmentation, the C-H repulsive energy will be channeled into translational energy of H and C in inverse ratio to their masses. Most of the energy will go to H translation and very little to C where it would appear as HC-C vibration [16]. We feel comfortable in assuming, then, that some ground state $C_2H$ is produced; of course, we cannot be certain this is true so our derived bond energy will have to be an upper limit. The fast edge of our $P(E_T)$ has $E_T$ = 17.5 kcal/mole which would correspond to a bond energy of 130.5 kcal/mole. Comparing our $P(E_T)$ with that of Wodtke and Lee, however, shows that this

fast edge has contamination from hot $C_2H_2$ photodissociation [4]. Instead of trying to guess where the ground state $C_2H_2$ dissociation starts contributing, we decided to make use of the recent work identifying $C_2H$ vibrational and electronic states. We can determine the bond energy by matching our spectrum with the known $C_2H$ transitions. In doing this, we concentrated on the best resolved peaks (4 and 5). Since an inverted vibrational distribution with selective excitation of only two higher vibrational states of the ground electronic state is not expected, we assumed that these peaks were primarily from the formation of electronically excited $C_2H$ in the A state. The main uncertainty in the fitting (~ ± .5 kcal/mole) comes in deciding how much rotational excitation there is -- how far to offset the assignment from the peak in the TOF spectrum. Table II and Figure 11 [37,38,39,40,41,42,43,44] show what we judge to be the best fit.

Assuming we have correctly matched the peaks and that we are not off by a quantum number in assigning the bending vibrational state, the $C_2H$ ground state is formed at $E_T$ = 16.5 kcal/mole. $D_0$(HCC-H) then would be 131.5 ± .5 kcal/mole. We could be more confident in this assignment if we could explain what the other peaks we see are and why those who studied $C_2H$ did not detect all the states we seem to.

The close spacing of the unidentified peaks suggests that they might be from bending vibrations. In Kanamori's $C_2H$ studies, they could not tell for certain if the peak at 2166 $cm^{-1}$

was from $C_2H$ $\nu_2$ = 7 (0 7 0)←(0 0 0) or $\nu_2$ = 5 (0 5 0)←(0 0 0), although they argued that the $\nu_2$ = 7 assignment was more likely. If the former were true, they estimated an $\omega_e\chi_e$ = 10.1 $cm^{-1}$ and if the latter were true, $\omega_e\chi_e$ = -15.8 $cm^{-1}$ [40]. Using these anharmonic constants, we predicted the values for other bending overtones. The assumption that the peak at 2166 $cm^{-1}$ is from (0 7 0) and that $\omega_e\chi_e$ = 10.1 $cm^{-1}$ fits our observed spectrum quite well and would allow us to assign several other peaks. As can be seen from Figure 11, peak 2b would be from $\nu_2$ = 9 and 10 and peak 3 from $\nu_2$ = 11 and 12.

Peaks 2b and 3 are very real in our TOF spectrum yet no spectroscopists have assigned any $C_2H$ peaks in this region (3323 to 2273 $cm^{-1}$). It should be noted, however, that in Jacox and Olson's matrix isolation studies of $C_2H$ they saw unidentified peaks at 2544.3, 2647.6, 2943.1, and 3105.5 $cm^{-1}$ [42] which probably correspond to the peaks in our spectrum. The reason that the peaks have not been identified by spectroscopists is most likely because of the low transition probabilities associated with the states involved. Looking at the $C_2H$ peaks that have been identified, one can see that they are all close to some other more fundamental state: $\nu_2$=7 and $\nu_2+\nu_3$, A and $5\nu_2+\nu_3$, A and unknown, A and $\nu_2+2\nu_3$ and $\nu_1+\nu_2$. Perhaps, then, the bends we think we see have not previously been identified because they are multiple quanta transitions and are not close enough to any other states to gain oscillator strength.

Knowing what states the peaks of the $P(E_T)$ correspond to

gives us some information about the dynamics of the photodissociation process. Although it is impossible to get relative weights for the states that form because of the extensive overlap, the general trend is that the $C_2H$ with large amount of internal excitation (8 to 13 kcal/mole) is preferentially formed. The C-H bend is highly excited (at least up to $\nu_2 = 12$) and both the C-C C-H stretches are excited. The first $C_2H$ electronic state, $A^1\Pi_u$, is also reached. As discussed, the large amount of vibrational excitation is expected (especially the C-H bend and C-C stretch) since there are large changes in the C-C-H bond angle and C-C distance during the dissociation. It is also not surprising to find that the A state is formed since at 193 nm the $C_2H_2$ is excited to the $1^1A''$ state ($C_s$ symmetry) which correlates with $C_2H(A) + H$. In fact, to explain the formation of $C_2H(X)$, one must invoke surface hopping at a $2^1A'/1^1A'$ or a $2^3A'/1^3A'$ avoided crossing [4,45].

One interesting question is the cause of the bumps in the $P(E_T)$ at $E_T > 7$ kcal/mole. Assuming the $\omega_e\chi_e = 10.1$ cm$^{-1}$ for $\nu_2$, the C-H bend, there is not one such bump per peak as might be expected. There are two possible explanations. The bumps could be from some "interference" in forming X(0 N 0) and X(0 N 1). The other possibility is that even bends are favored as a consequence of the $C_2H_2$ fragmenting in plane. If the dissociation is confined to a plane, conservation of angular momentum prevents the $C_2H$ from being produced with angular momentum about the C-C bond which means only $C_2H$ with an even

quanta of bending vibration can form [4].

The previous discussion was based on our assumption that ground state $C_2H$ does form. What if we do not make this a requirement and try to see if our $P(E_T)$ can be fit with some lower bond energies? These fits, shown in Figure 12, are not as satisfying as our $D_0$ = 131.5 kcal/mole fit for several reasons. First, all the fits leave a peak unassigned. Jacox and Olson, however, have seen lines associated with $C_2H$ in these regions [42] so this is not an entirely convincing argument. A more damaging point is that these fits would require a highly specific and inverted vibrational distribution. For example, assuming $D_0$ = 127.7 kcal/mole, would assign the three strongest peaks to high X levels (> X(1 1 0) and X(0 1 2)) and/or high A levels (> A(0 1 0)). While we would not be surprised to find highly vibrationally excited product, such an inversion would not be expected. Finally, the fits at these lower bond energies are not as good. For $D_0$ = 130.5 and 127.7 kcal/mole, X(0 7 0), X(0 1 1), and X(0 0 1) do not match any peaks. This can not be easily explained by invoking rotational excitation since not much is expected.

**b. Secondary Dissociation**

Assuming that primarily $C_2H$ with internal energy of 9.5 to 13.5 kcal/mole (products with 3 to 7 kcal/mole in translation) will undergo secondary dissociation to $C_2$ + H($^2$S) and that the H-CC bond energy is 116 kcal/mole [9], the two peaks in the secondary $P(E_T)$ indicate that the $C_2$ forms with $E_{Int}$ = 20-28 (peak

1) and 32-40 kcal/mole (peak 2). Unfortunately, because of the nature of $C_2H$ secondary dissociation, our TOF spectra are not sensitive enough to tell unambiguously what $C_2$ states form. The spectra, however, do reveal some general features of the dissociation process.

One conclusion that can be drawn from the secondary dissociation fitting is that $C_2H$ must have an $E_{Int}$ of $\geq$ 9.5 kcal/mole to photodissociate further. This value suggests that only $C_2H$ in the upper electronic A state and/or highly vibrationally excited ground state can absorb a photon and fragment. This would agree with the theoretical predictions of what $C_2H$ electronic transitions are accessible to a 193 nm photon. As discussed, to reach the lowest allowed electronic states would require that the $C_2H$ have a non-equilibrium C-C bond length and/or be nonlinear.

The overall appearance of the secondary $P(E_T)$ is reliable and offers some insight to the dissociation process. At all laser powers, very little ground state $C_2$ seems to be produced; most of the $C_2$ is formed highly excited. This is probably because of the large number of $C_2$ electronic states available for the $C_2H^*$ to cross into. In addition, since there is no reason to expect a bimodal vibrational distribution, it is reasonable to assume that peaks 1 and 2 result from the production of different electronic species. Peak 2 is most likely $B^1\Delta_g$ with the slow tail being higher vibrational levels of $c^3\Sigma_u^+$. The fast edge of peak 1 could be from $b^3\Sigma_g^-$ and the slow edge from $A^1\Pi_u$.

The $C_2$ electronic states that appear to form in the 193 nm secondary dissociation of $C_2H_2$ have been seen before (except the $c^3\Sigma_u^+$ state). The new information our results provide is that more of the highly excited $C_2$ states (B and c) form than A, a, or X. Like us, Wodtke and Lee saw more highly excited product ($E_T$ = 10 kcal/mole) but both our peak positions and our assignments differ [4]. Possible reasons for this are that they used a cruder treatment of secondary dissociation, they used a different $P'(E_T)$, or they used different thermodynamic values. The uncertainties in the secondary dissociation fitting make it unlikely that the TOF method could be used to determine the $C_2$ states that form. Our experiment only suggests that higher $C_2$ states than Wodtke and Lee inferred may be forming and that these states are preferentially produced over less electronically excited states.

## 5. CONCLUSION

To confirm our group's previous measurement of the HCC-H bond energy, we used the same approach, 193 nm photofragmentation translational spectroscopy, but detected the H atom. This detection scheme has several advantages -- the measurements can be well calibrated, the data can be collected at one lab angle, and the TOF spectra are not affected by small variations in the parent beam. We also have the advantage of several years of research on $C_2H$ vibrational and electronic states to help us determine the threshold translational energy of ground state $C_2H$

from the structure of the translational energy distribution rather than having to guess where the signal from the dissociation of vibrationally excited $C_2H_2$ ends. These improvements give us confidence in the dissociation energy we found, 131.5 ± .5 kcal/mole. The bond energy we measured agrees with our group's previous attempt and is in the range of the latest experimental and theoretical predictions so adds more support to the $D_0$(HCC-H) > 130 kcal/mole "side". We see no evidence of the faster H atoms from the primary dissociation process detected in Segall, et. al.'s experiment.

Although our H atom TOF spectra do not have nearly the resolution found in the $C_2H$ absorption spectroscopy studies, we have the advantage of being able to see $C_2H$ states that lack oscillator strength. Our results support Kanamori and Hirota's assignment of their 2166 $cm^{-1}$ peak to (0 7 0) with an $\omega_e\chi_e$ = 10.1 $cm^{-1}$. We also observe structure that we hypothesize is due to C-H bending vibration in the range of some of Jacox and Olson's unassigned peaks.

Finally, our TOF study adds to the understanding of the 193 nm photodissociation dynamics of acetylene. Comparison to the known $C_2H$ spectrum shows that we formed both $C_2H$ A and X which is only possible if curve-crossing is important in the system. As expected from the large geometry changes involved, we see high vibrational levels of $C_2H$ X and A. There also might be a preference for bending vibrations with the even quanta of excitation which is reasonable if it is assumed that the $C_2H_2$

dissociates in plane. In addition to the primary photodissociation, our results increase what is known about the two photon sequential dissociation, $C_2H_2 \rightarrow C_2H + H \rightarrow C_2 + H + H$. Highly excited $C_2H$ molecules preferentially dissociate as theoretically predicted. Also, the formation of electronically excited $C_2$ seems to be favored probably because of the large density of these states near the second photon energy.

**ACKNOWLEDGMENTS**

We would like to thank Prof. W.M. Jackson for his useful discussions on the primary and secondary photochemistry processes and for providing a preprint of his group's experimental results. We also acknowledge helpful discussions on our experimental techniques and set-up with Dr. R.E. Continetti. This work was supported by the Director, Office of Basic Energy Sciences, Chemical Sciences Division of the U.S. Department of Energy under contract No. DE-AC03-67SF00098.

Table I. Recent Determinations of $D_0$(HCC-H)

| Year | $D_0$(HCC-H) (kcal/mole) | Technique | Ref. |
|---|---|---|---|
| 1990 | 131.5 ± .5 | H atom (mass spec) velocity after dissociation | this work |
| 1990 | 131 ± 1 | H atom (REMPI) velocity after dissociation | 11 |
| 1990 | 131.6 ± 1 | $C_2H^-$ + $H^+$ threshold thermochem. cycle | 10 |
| 1990 | 131.3 ± .7 | radical electron affinity (photoelectron spec) + gas phase acidity thermochem cycle | 9 |
| 1990 | 129.7 | theory | 15 |
| 1990 | 130.1 ± 1 | theory | 14 |
| 1990 | 131.54 ± .51 | theory | 13 |
| 1989 | 126.647 ± .002 | SAC | 8 |
| 1989 | ≤ 127 ± 1.5 | H atom Doppler shifts after dissociation | 7 |
| 1989 | 133.52 ± 2.3 | theory | 12 |
| 1988 | ≤ 132.3 ± .001 | SEP with ZAC | 6 |
| 1987 | 132.6 ± 1 | $C_2H$ + $H^+$ + $e^-$ threshold thermochem. cycle | 5 |
| 1985 | 132 ± 2 | $C_2H$ velocity after dissociation | 4 |

Table II. Compilation of observed $C_2H$ states and their positions in our $P(E_T)$

| TOF Peak | Exp. Trans. ($cm^{-1}$) | Assignment | Ref. |
|---|---|---|---|
| | 5543 | X | 37,38 |
| | 5403 | | |
| | 5161 (from 3320 + $\nu_3$) | | 37 |
| 5 | 4144 | A(0 1 0) | |
| | 4108 | X(0 1 2) | 18,38,39 |
| | 4012 | X(1 1 0) | |
| 4 | 3786 | X(0 5 1) | 18,39 |
| | 3693 | A(0 0 0) | 18,39,40 |
| | 3600 | ? ← X(0 0 0) | 37,38,40 |
| | 3547 | | |
| | 3366 | | 41 |
| | 3299 | | |
| 3 | 3105.5 | ? ← X(0 0 0) | 42 |
| | 2943.1 | | |
| 2b | 2647.6 | ? ← X(0 0 0) | 42 |
| | 2544.3 | | |
| 2a | 2166 | X(0 7 0) | 40 |
| | 2091 | X(0 1 1) | 43 |
| | 1841 | X(0 0 1) | 44 |
| 1 | 372 | X(0 1 0) | 40 |

**REFERENCES**


1. M.B. Colket III, Twenty-First Symposium (International) on Combustion (Combustion Institute, Pittsburgh, 1986), p. 851; C.K. Westbrook and F.L Dryer, Eighteenth Symposium (International) on Combustion (Combustion Institute, Pittsburgh, 1981), p. 749; H. GG. Wagner, Seventeenth Symposium (International) on Combustion (Combustion Institute, Pittsburgh, 1979), p. 3.

2. T. Tanzawa and W.C. Gardiner Jr., Seventeenth Symposium (International) on Combustion (Combustion Institute, Pittsburgh, 1979), p. 564.

3. A.M. Wodtke and Y.T. Lee, Advances in Gas Phase Photochemistry and Kinetics: Molecular Photodissociation Dynamics, edited by M.N.R. Ashfold and J.E. Baggott (Royal Society of Chemistry, London, 1987), p. 31.

4. A.M. Wodtke and Y.T. Lee, J. Phys. Chem. **89**, 4744 (1985); A.M. Wodtke, Ph.D. Thesis, University of California, Berkeley, 1986.

5. H. Shiromaru, Y. Achiba, K. Kimura, and Y.T. Lee, J. Phys. Chem. **91**, 17 (1987).

6. Y. Chen, D.M. Jonas, C. E. Hamilton, P.G. Green, J.L. Kinsey, and R.W. Field, Ber. Bunsenges. Phys. Chem. **92**, 329 (1988).

7. J. Segall, R. Lavi, Y. Wen, and C. Witting, J. Phys. Chem. **93**, 7287 (1989).

8. P.G. Green, J.L. Kinsey, and R.W. Field, J. Chem. Phys. **91**, 5160 (1989).

9. K.M. Ervin, S. Gronert, S.E. Barlow, M.K. Gilles, A.G. Harrison, V.M. Bierbaum, C.H. DePuy, W.C. Lineberger, and G.B. Ellison, J. Am. Chem. Soc. **112**, 5750 (1990).

10. B. Ruscic and J. Berkowitz, J. Chem. Phys. **93**, 5586 (1990).

11. D.P. Baldwin, M.A. Buntine, and D.W. Chandler, J. Chem. Phys. **93**, 6578 (1990).

12. L.A. Curtiss and J.A. Pople, J. Chem. Phys. **91**, 2420 (1989).

13. J.A. Montgomery Jr. and G.A. Petersson, Chem. Phys. Lett., **168**, 75 (1990).

14. C.W. Bauschlicher Jr., S.R. Langhoff, and P.R. Taylor, Chem. Phys. Lett. **171**, 42 (1990).

15. C.J. Wu and E.A. Carter, J. Am. Chem. Soc. **112**, 5893 (1990).

16. G.E. Busch and K.R. Wilson, J. Chem. Phys. **56**, 3626 (1972).

17. For a discussion of complexities see, for example, H. Thümmel, M. Perić, S.D. Peyerimhoff, and R.J. Buenker, Z. Phys. D. - Atoms, Molecules, and Clusters **13**, 307 (1989).

18. R.F. Curl, P.G. Carrick, and A.J. Merer J. Chem. Phys. **82**, 3479 (1985).

19. P.D. Foo and K.K. Innes, Chem. Phys. Lett. **22**, 439 (1973).

20. C.K. Ingold and G.W. King, J. Chem. Soc. 2702 (1953).

21. K.K. Innes, J. Chem. Phys. **22**, 863 (1954).

22. M. Douay, R. Nietmann, and P.F. Bernath, J. Mol. Spectrosc. **131**, 261 (1988).

23. K.P. Huber and G. Herzberg, Molecular Spectra and Molecular Structure: IV. Constants of Diatomic Molecules (Van Nostrand Reinhold Company, New York, 1979).

24. M.W. Chase Jr., C.A. Davies, J.R. Downey Jr., D.J. Frurip, R.A. McDonald, and A.N. Syverud, JANAF Thermochemical Tables, Third Edition (Journal of Physical and Chemical Reference Data, New York, 1986).

25. T.R. Fletcher and S.R. Leone, J. Chem. Phys. **90**, 871 (1989).

26. J.R. McDonald, A.P. Baronavski, and V.M. Donnelly, Chem. Phys. **33**, 161 (1978).

27. R.S. Urdahl, Y. Bao, and W.M. Jackson, Chem. Phys. Lett. **152**, 485 (1988).

28. P.M. Goodwin and T.A. Cool, J. Mol. Spectrosc. **133**, 230 (1989).

29. Y. Bao, R.S. Urdahl, and W.M. Jackson - preprint.

30. S. Shih, S.D. Peyerimhoff, and R.J. Buenker, J. Mol. Spectrosc. **64**, 167 (1977).

31. S. Shih, S.D. Peyerimhoff, and R.J. Buenker, J. Mol. Spectrosc. **74**, 124 (1979).

32. Y.T. Lee, J.D. McDonald, P.R. LeBreton, and D.R. Herschbach, Rev. Sci. Inst. **40**, 1402 (1968); R.K. Sparks, Ph.D. Thesis, University of California, Berkeley (1979).

33. R.E. Continetti, B.A. Balko, and Y.T. Lee, J. Chem. Phys. **93**, 5719 (1990); R.E. Continetti, Ph.D. Thesis, University of California, Berkeley (1989).

34. L.J. Kieffer, Atomic Data **1**, 19 (1969).

35. X. Zhao, Ph.D. Thesis, University of California, Berkeley (1988).

36. R.D. Levine and R.B. Bernstein, Molecular Dynamics and Chemical Reactivity (Oxford University Press, New York, 1987).

37. W.-B. Yan, J.L. Hall, J.W. Stephens, M.L. Richnow, and R.F. Curl, J. Chem. Phys. **86**, 1657 (1987).

38. M. Vervloet and M. Herman, Chem. Phys. Lett. **144**, 48 (1988).

39. P.G. Carrick, A.J. Merer, and R.F. Curl Jr., J. Chem. Phys. **78**, 3652 (1983).

40. H. Kanamori and E. Hirota, J. Chem. Phys. **89**, 3962 (1988).

41. J.W. Stephens, W.-B. Yan, M.L. Richnow, H. Solka, and R.F. Curl, J. Mol. Struct. **190**, 41 (1988).

42. M.E. Jacox and W.B. Olson, J. Chem. Phys. **86**, 3134 (1987).

43. K. Kawaguchi, T. Amano, and E. Hirota, J. Mol. Spectrosc. **131**, 58 (1988).

44. H. Kanamori, K. Seki, and E. Hirota, J. Chem. Phys. **87**, 73 (1987).

45. T.A. Cool, P.M. Goodwin, and C.E. Otis, J. Chem. Phys. **93**, 3714 (1990).

**FIGURE CAPTIONS**

**Figure 1.** Product channels thermochemically possible in the 193 nm photodissociation of acetylene. The dashed, secondary dissociation lines represent the energy limits if the ground state or the most internally excited $C_2H$ absorbs a photon. The heats of formation and bond energies used to construct this chart are from references 9, 22, 23, and 24.

**Figure 2.** Side-view (a) and top-view (b) of the experimental arrangement. The piezo-electric pulsed valve (1) is used to create a beam of $C_2H_2$. The valve fires into the photolysis chamber (2). The beam passes through a skimmer (3) in the high resolution mode. A 4" DP (4) as well as liquid nitrogen cooled cryopanels (5) pump the chamber. The output of the excimer laser (6) passes through a focusing lens (7) and perpendicularly intersects the acetylene beam (8). The photoproducts (9) pass out the differential chamber and travel 39.0 cm to the detector (10) where they can be ionized in the electron impact ionizer (11). A chopping wheel (12) is used to gate the detector to help reduce the background.

**Figure 3.** (a) Kinematic diagram for our experiment showing the H atom product velocity. 16 kcal/mole is the translational energy of the fastest $C_2H$ + H products and 3 kcal/mole is the lower limit for most of the observed product. The diagram shows that since we detect 90° from the parent beam we cannot see even the fastest $C_2H$ product (or any product with a COM velocity slower than the parent beam). (b) Kinematic diagram for Wodtke and Lee's experiment where they detected the $C_2H$ fragment. Comparison of the two diagrams shows that our experiment will be much less affected by variations in the parent beam.

**Figure 4.** Representative high resolution TOF spectrum showing the raw data (open circles) as well as the polynomial fit to the laser-off signal (solid line). This background correction has very little effect on the region of interest.

**Figure 5.** Representative high resolution TOF spectrum showing the raw data (open circles) with the RF pickup noise spectrum (solid line).

**Figure 6.** HI and DI calibration H (or D) atom TOF spectra. The two peaks in each spectrum are due to the formation of $I(^2P_{3/2})$ and $I(^2P_{1/2})$. Open circles are the raw data and the solid line is the calculated fit. (a) Photodissociation of HI in low resolution mode. (b) Photodissociation of HI in high resolution mode. (c) Photodissociation of DI in high resolution mode (note the change in time scale).

**Figure 7.** High resolution spectra. Open circles are the raw data (after background corrections) and solid line is the calculated best fit. Dashed line represents H atoms from

secondary dissociation. (a) Low power, 35 mj/pulse. (b) High power, 100-150 mj/pulse.

**Figure 8.** (a) Product translational energy distribution used to fit TOF spectrum in Figure 7b. (b) Wodtke and Lee's product translational energy distribution that gives the best fit to their $C_2H$ TOF spectra.

**Figure 9.** Low resolution TOF spectra. Open circles are the raw data, solid lines are the calculated best fit, and dashed lines are the secondary dissociation contribution. (a) 60 mj/pulse. (b) 105 mj/pulse. (c) 235 mj/pulse.

**Figure 10.** Secondary dissociation product translational energy distribution used to calculate the best fit in Figure 9c. The blocks represent where the ground vibrational level of the $C_2$ electronic states should appear assuming $C_2H$ with an internal energy of 9.5 - 13.5 kcal/mole ($E_T$ = 3 - 7 kcal/mole) dissociates.

**Figure 11.** Correspondence between known $C_2H$ states (see Table II) and our product translational energy distribution. Solid lines are observed transitions (from ground state $C_2H$); those that have been assigned are labeled. Dashed lines are the calculated $C_2H$ C-H bending vibrations assuming Kanamori and Hirota's 2166 $cm^{-1}$ is X(0 7 0) and $\omega_e\chi_e$ = 10.1 $cm^{-1}$. As can be seen, $C_2H$ X(0 0 0) is expected at $E_T$ = 16.5 kcal/mole which would give a $D_0$(HCC-H) = 131.5 ± .5 kcal/mole.

**Figure 12.** Comparison of fits of $C_2H$ spectrum to H atom TOF spectrum assuming a HCC-H bond energy of (a) 127.7 kcal/mole, (b) 128.8 kcal/mole, (c) 130.5 kcal/mole, and (d) 131.5 kcal/mole.

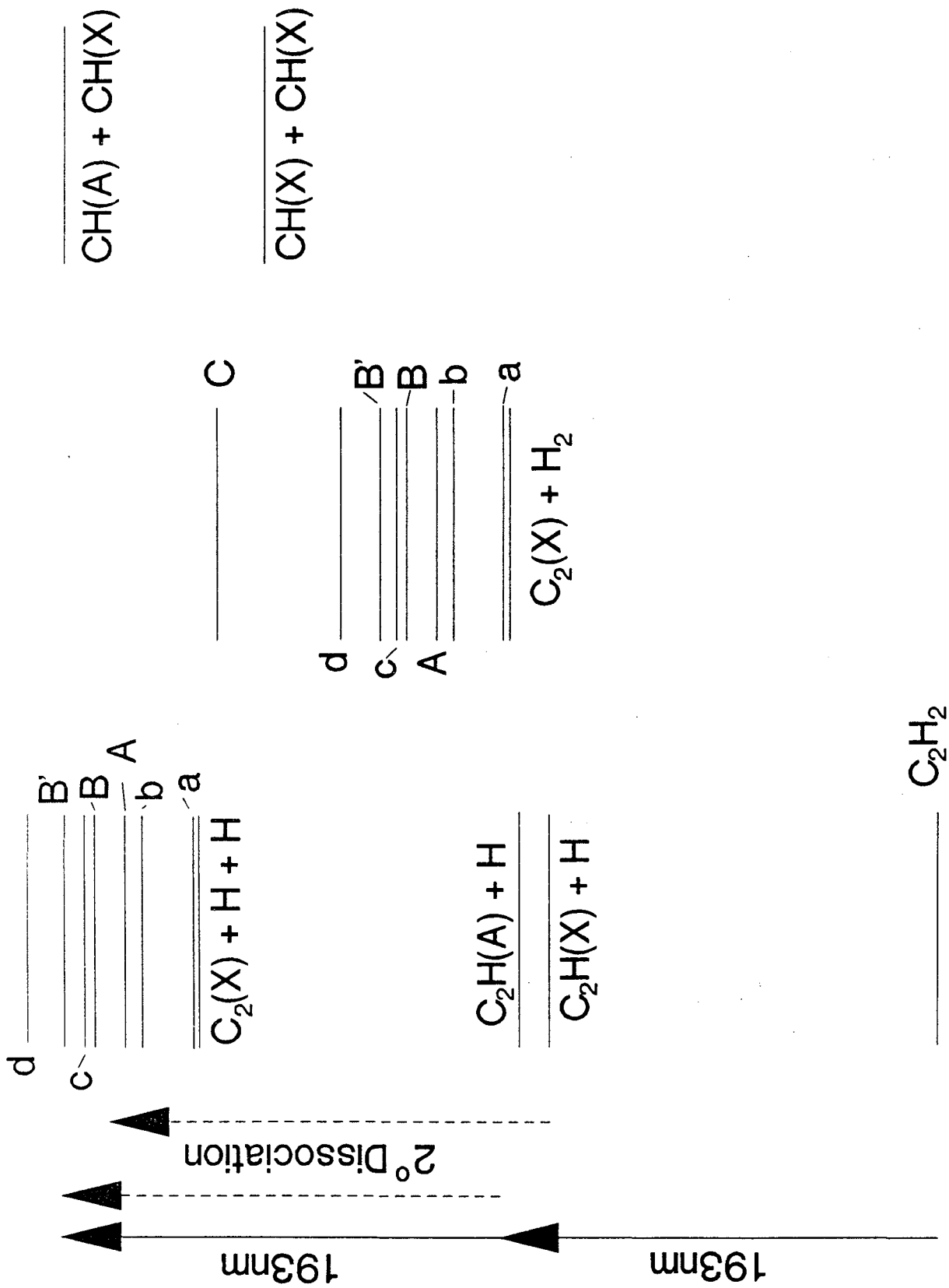
193nm
193nm
2° Dissociation
$C_2H_2$
$C_2H(X) + H$
$C_2H(A) + H$
$C_2(X) + H + H$
$C_2(X) + H_2$
CH(X) + CH(X)
CH(A) + CH(X)
a
b
A
B
B'
C
d
c'

Figure 1

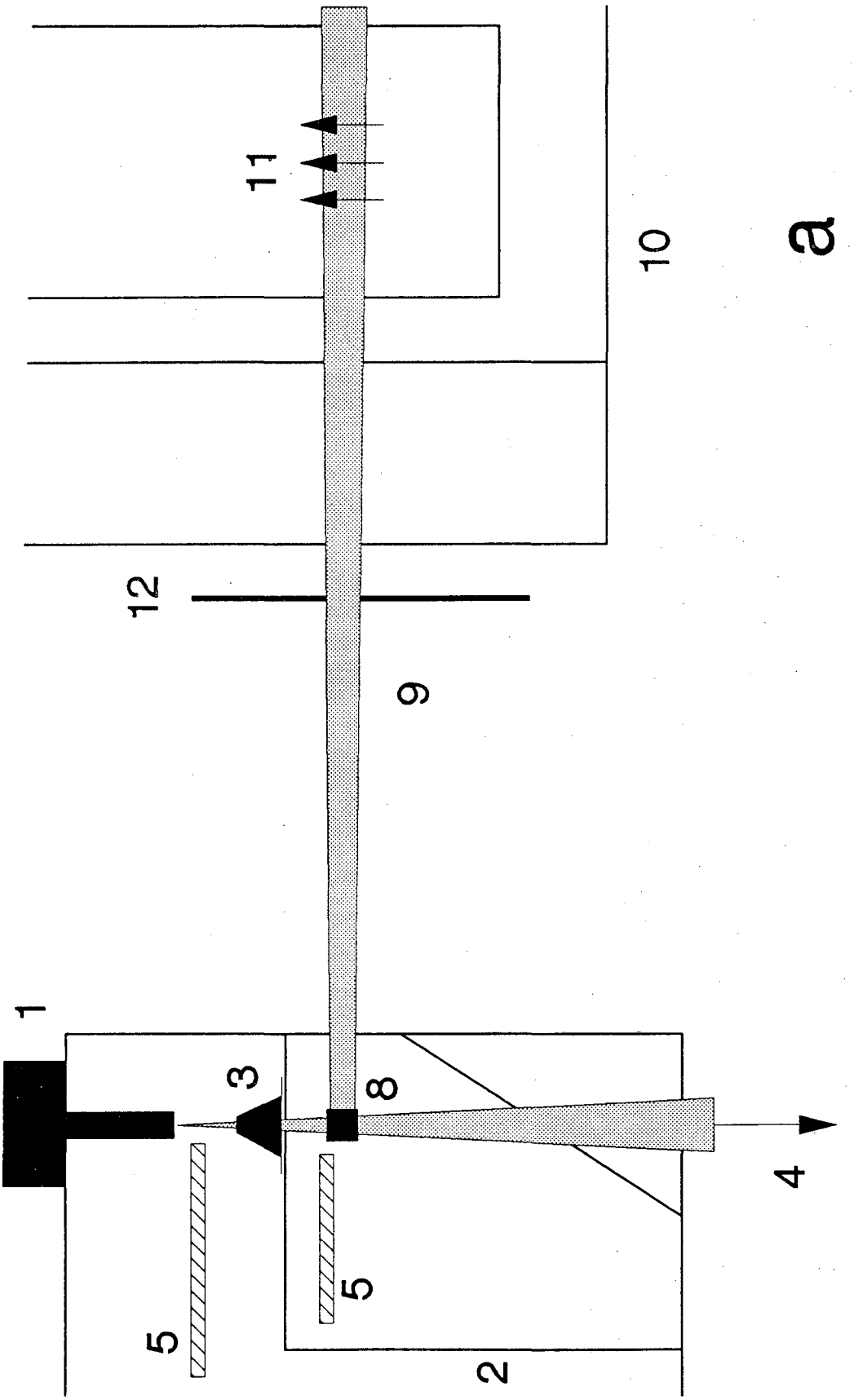


Figure 2a

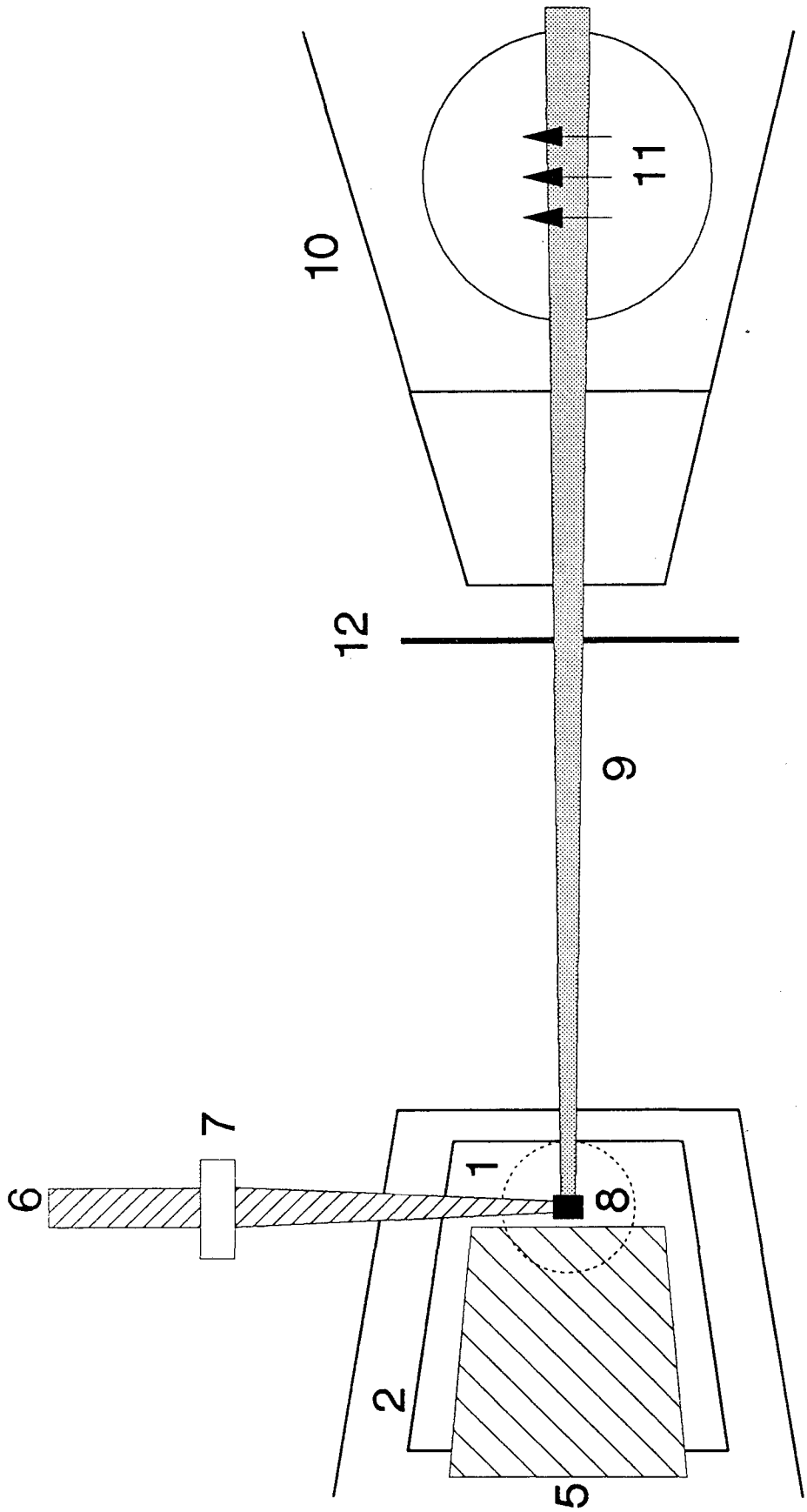


Figure 2b

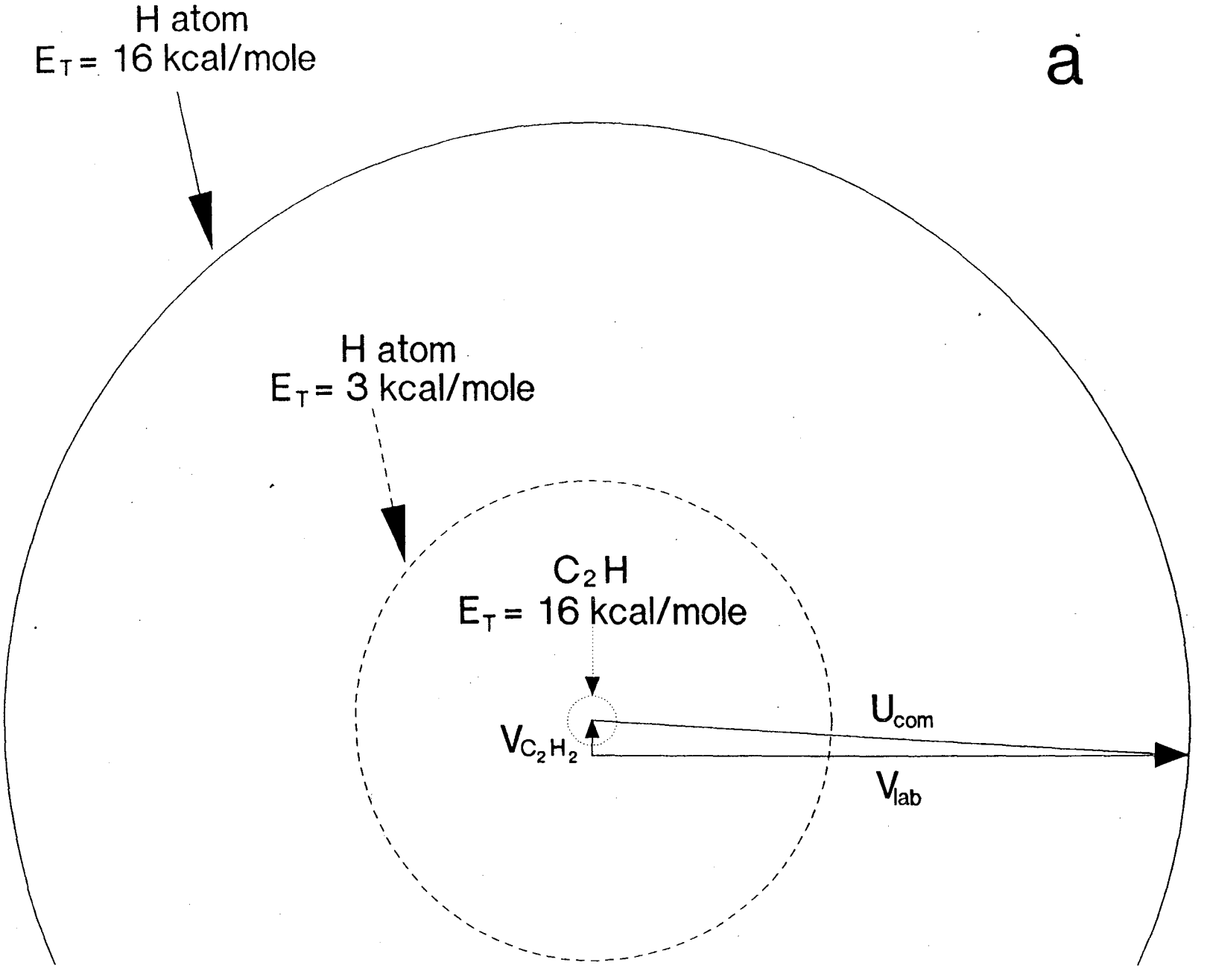
H atom
$E_T$ = 16 kcal/mole
a
H atom
$E_T$ = 3 kcal/mole
$C_2H$
$E_T$ = 16 kcal/mole
$V_{C_2H_2}$
$U_{com}$
$V_{lab}$

Figure 3a

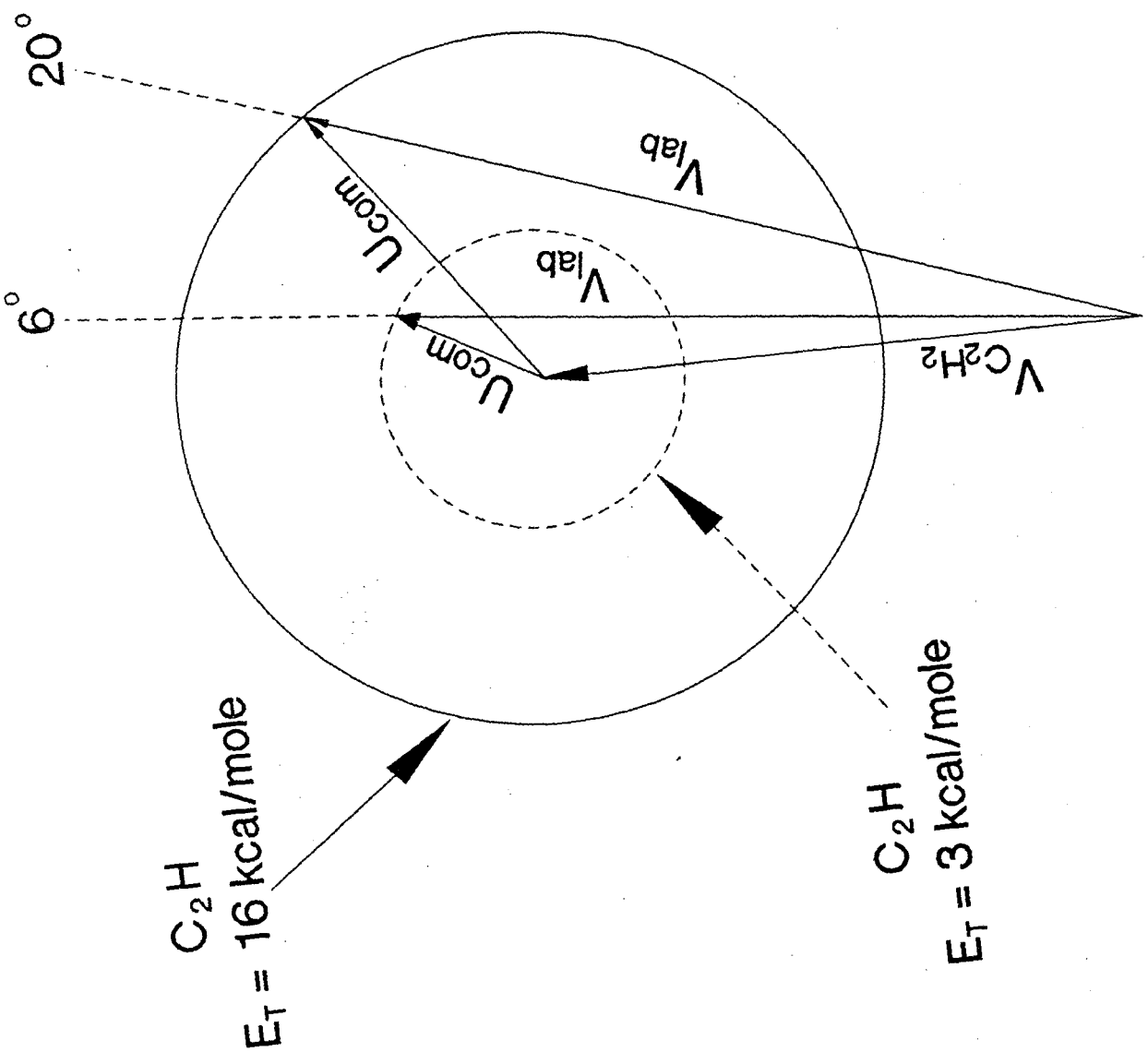
b
20°
6°
V lab
U com
V lab
U com
V C2H2
C2H
ET = 16 kcal/mole
C2H
ET = 3 kcal/mole

Figure 3b

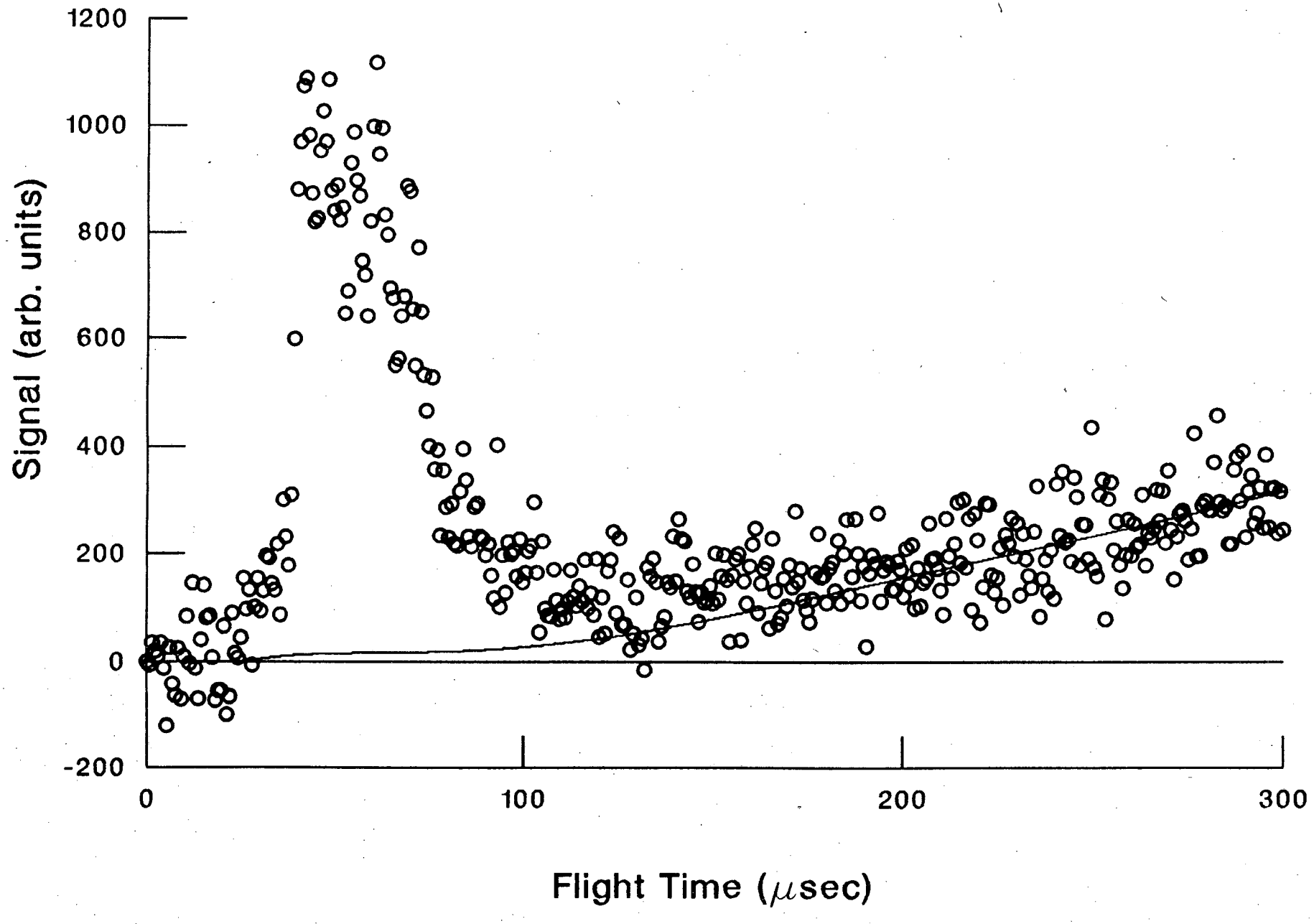
1200
1000
800
600
400
200
0
-200
Signal (arb. units)
0
100
200
300
Flight Time (μsec)

Figure 4

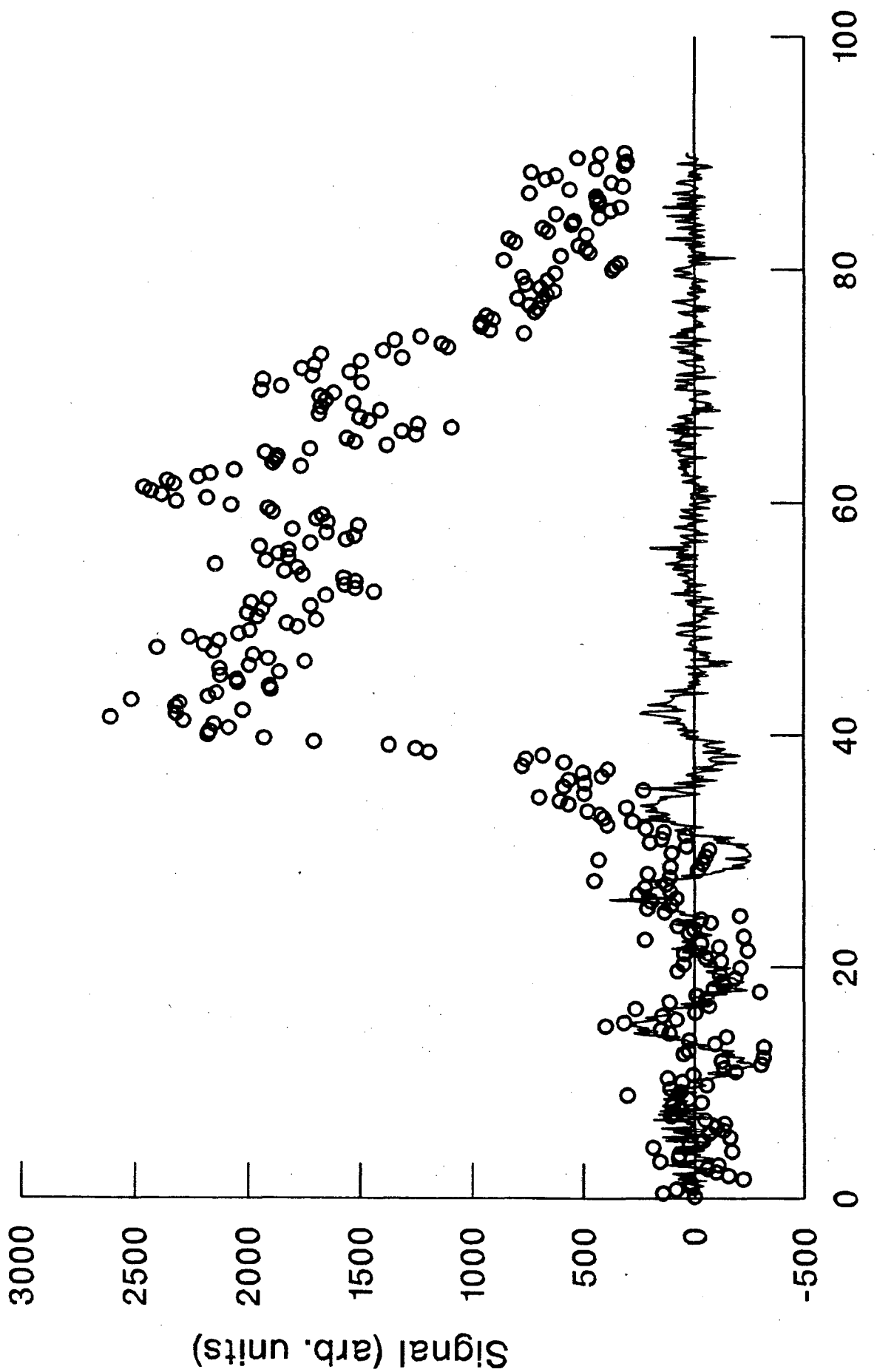
Signal (arb. units)
3000
2500
2000
1500
1000
500
0
-500
0
20
40
60
80
100
Flight Time (μsec)

Figure 5

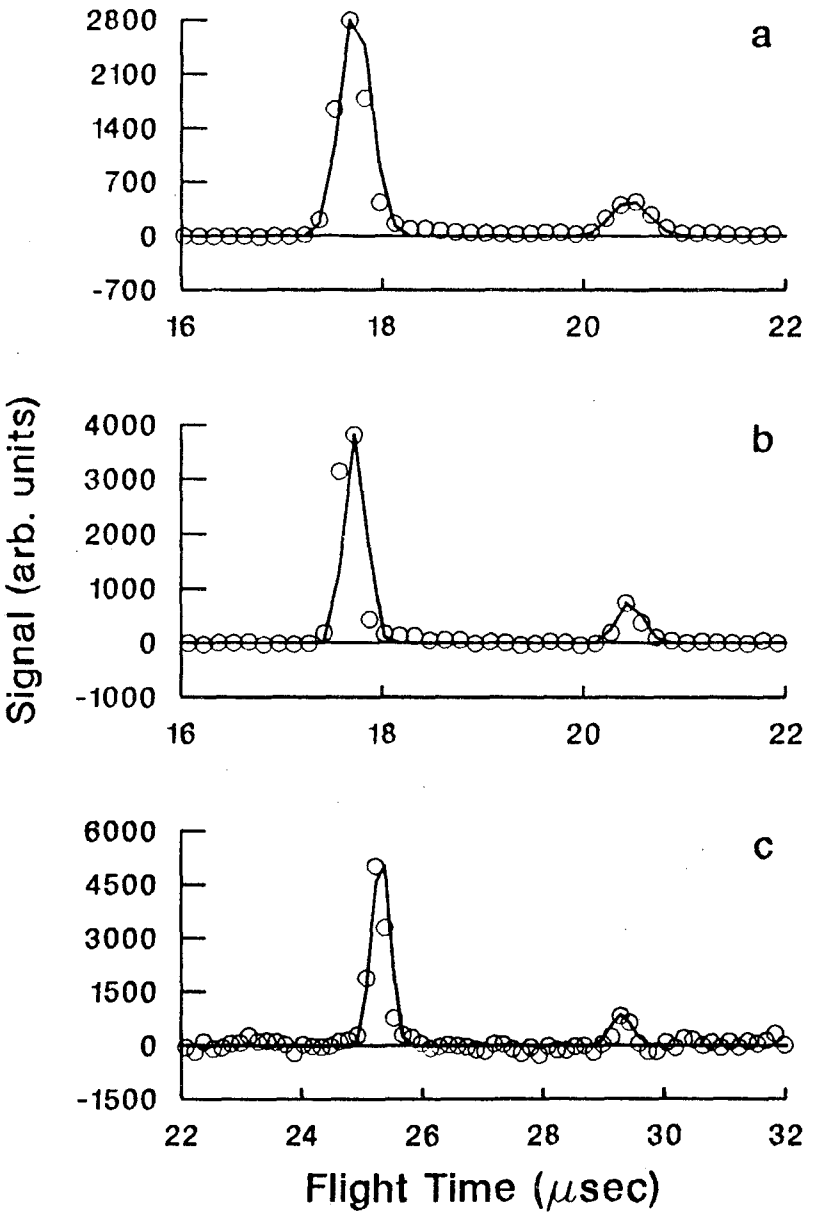
a
b
c
2800
2100
1400
700
0
-700
4000
3000
2000
1000
0
-1000
6000
4500
3000
1500
0
-1500
16
18
20
22
24
26
28
30
32
Signal (arb. units)
Flight Time (μsec)

Figure 6

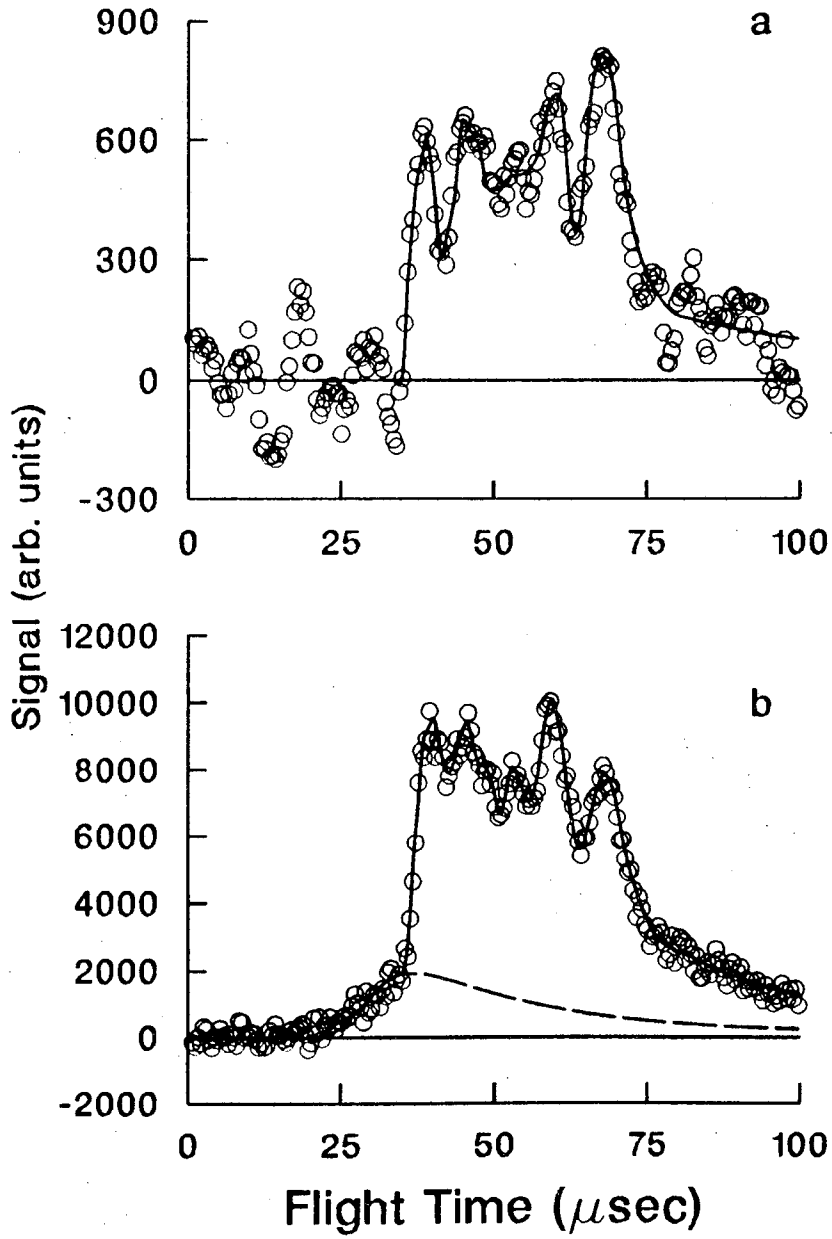
900
600
300
0
-300
a
0
25
50
75
100
12000
10000
8000
6000
4000
2000
0
-2000
b
0
25
50
75
100
Signal (arb. units)
Flight Time (μsec)

Figure 7

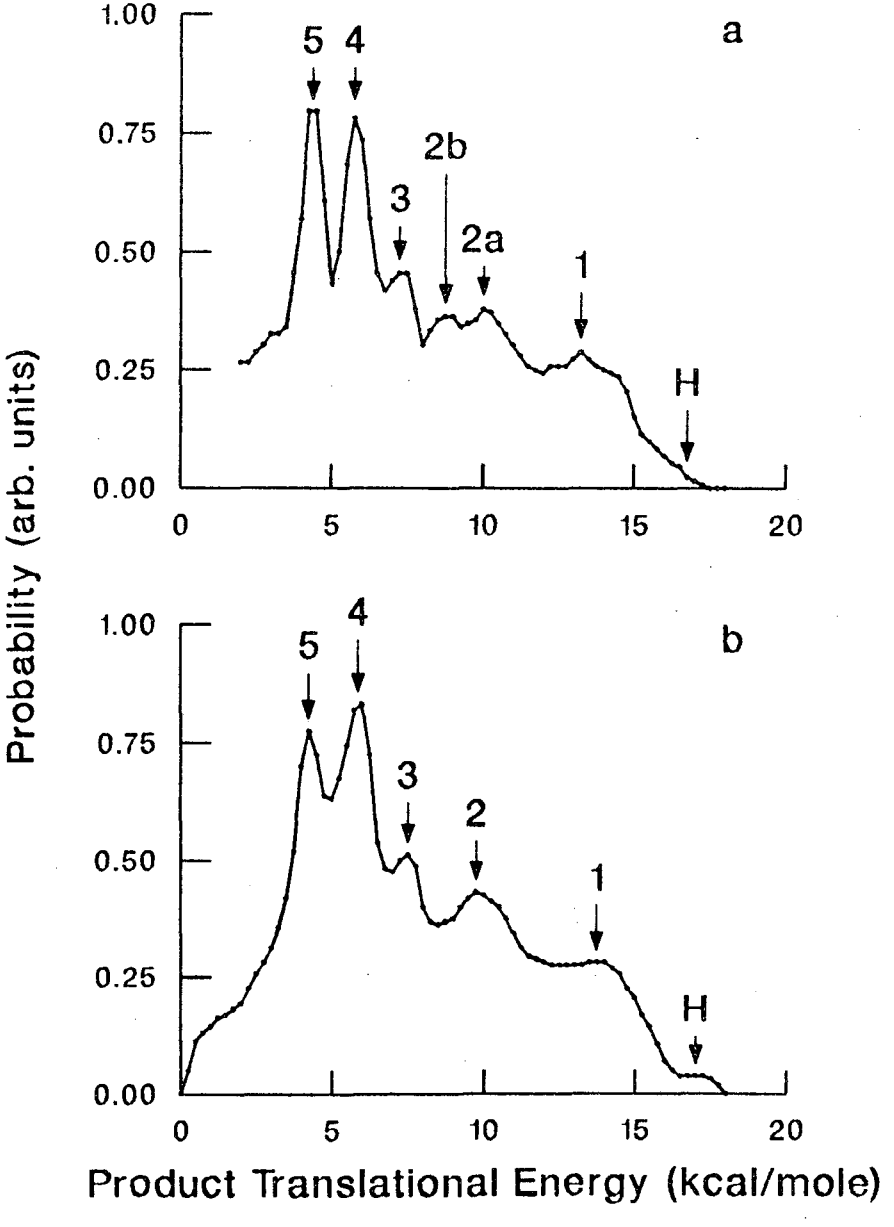
1.00
0.75
0.50
0.25
0.00
5
4
2b
3
2a
1
H
a
0
5
10
15
20
1.00
0.75
0.50
0.25
0.00
5
4
3
2
1
H
b
0
5
10
15
20
Probability (arb. units)
Product Translational Energy (kcal/mole)

Figure 8

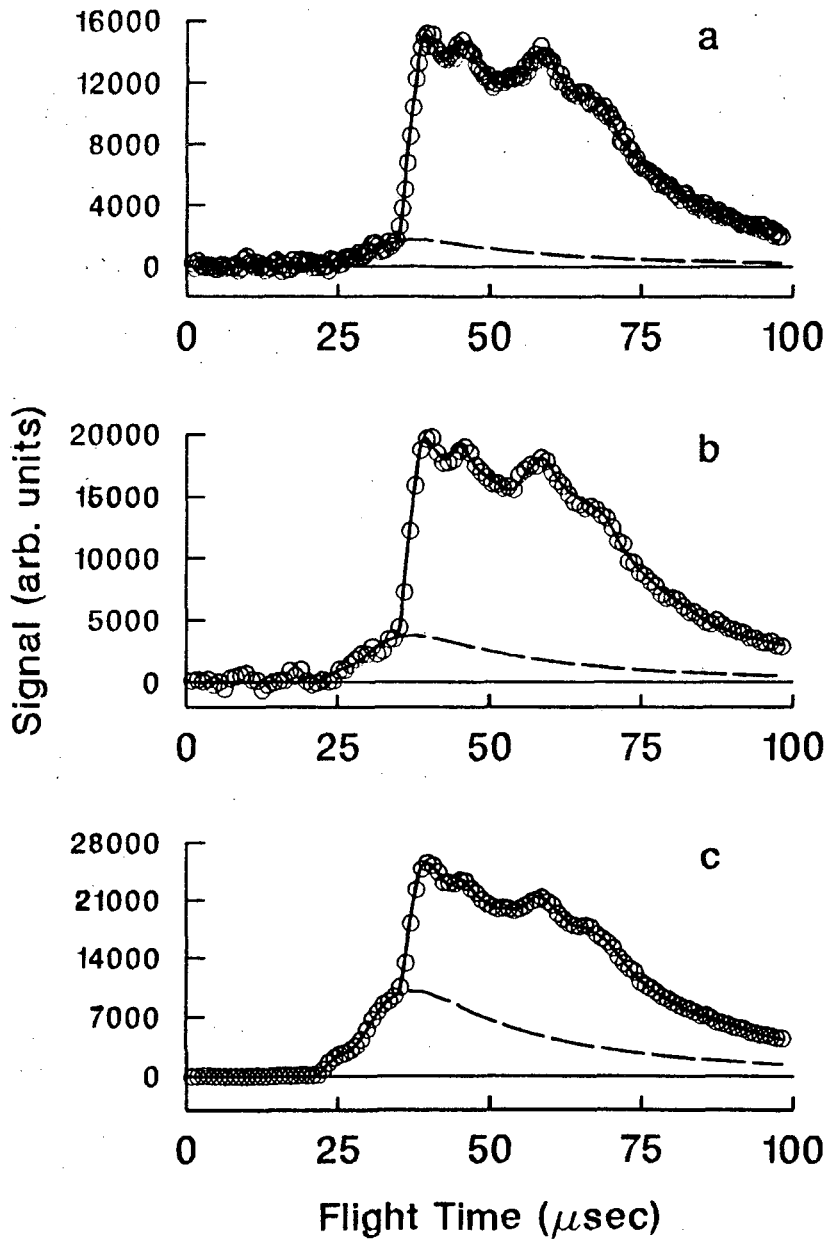
16000
12000
8000
4000
0
a
0
25
50
75
100
Signal (arb. units)
20000
15000
10000
5000
0
b
0
25
50
75
100
28000
21000
14000
7000
0
c
0
25
50
75
100
Flight Time (μsec)

Figure 9

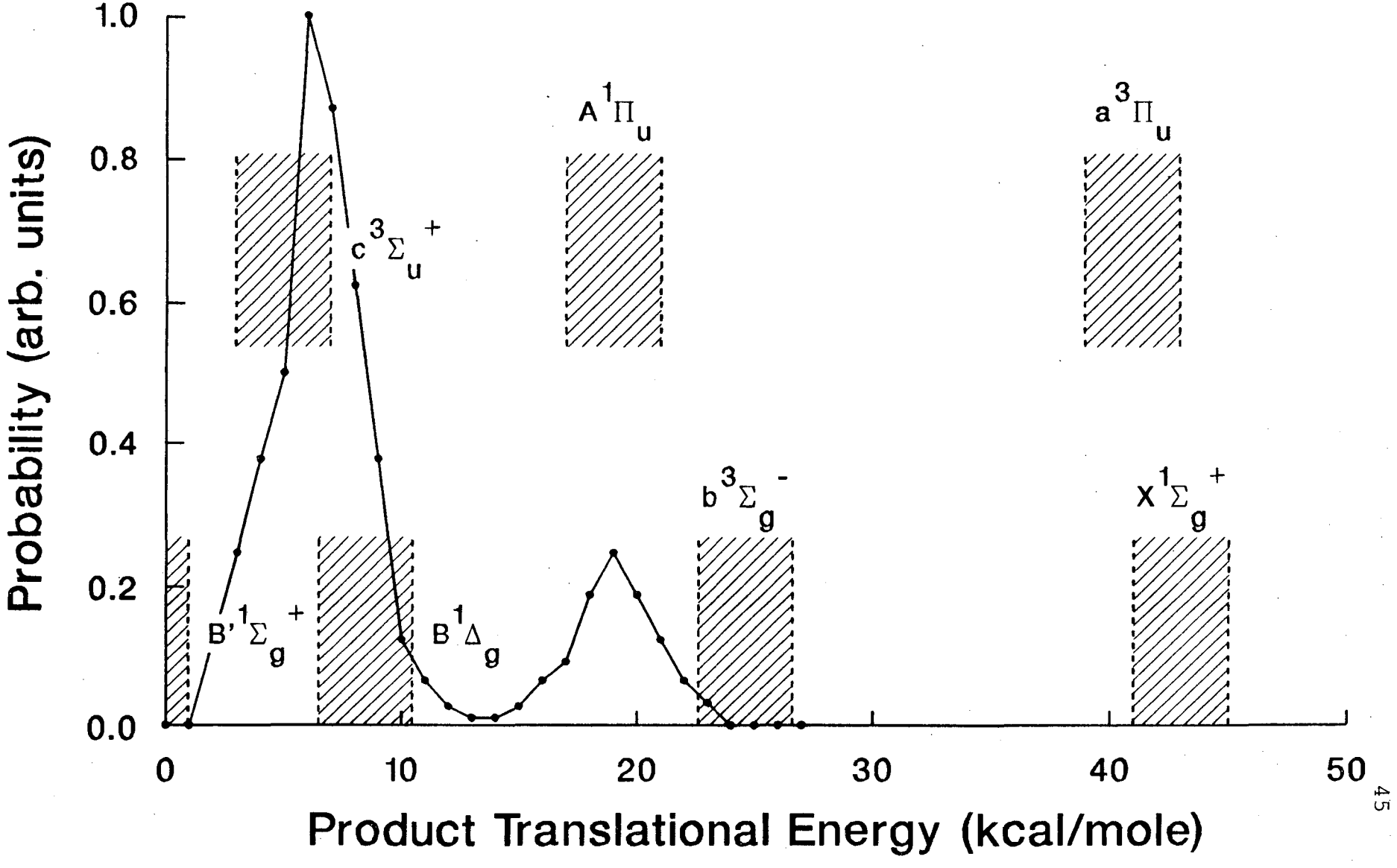
1.0
0.8
0.6
0.4
0.2
0.0
Probability (arb. units)
0
10
20
30
40
50
Product Translational Energy (kcal/mole)
$A\,^1\Pi_u$
$a\,^3\Pi_u$
$c\,^3\Sigma_u^+$
$b\,^3\Sigma_g^-$
$X\,^1\Sigma_g^+$
$B'\,^1\Sigma_g^+$
$B\,^1\Delta_g$

Figure 10

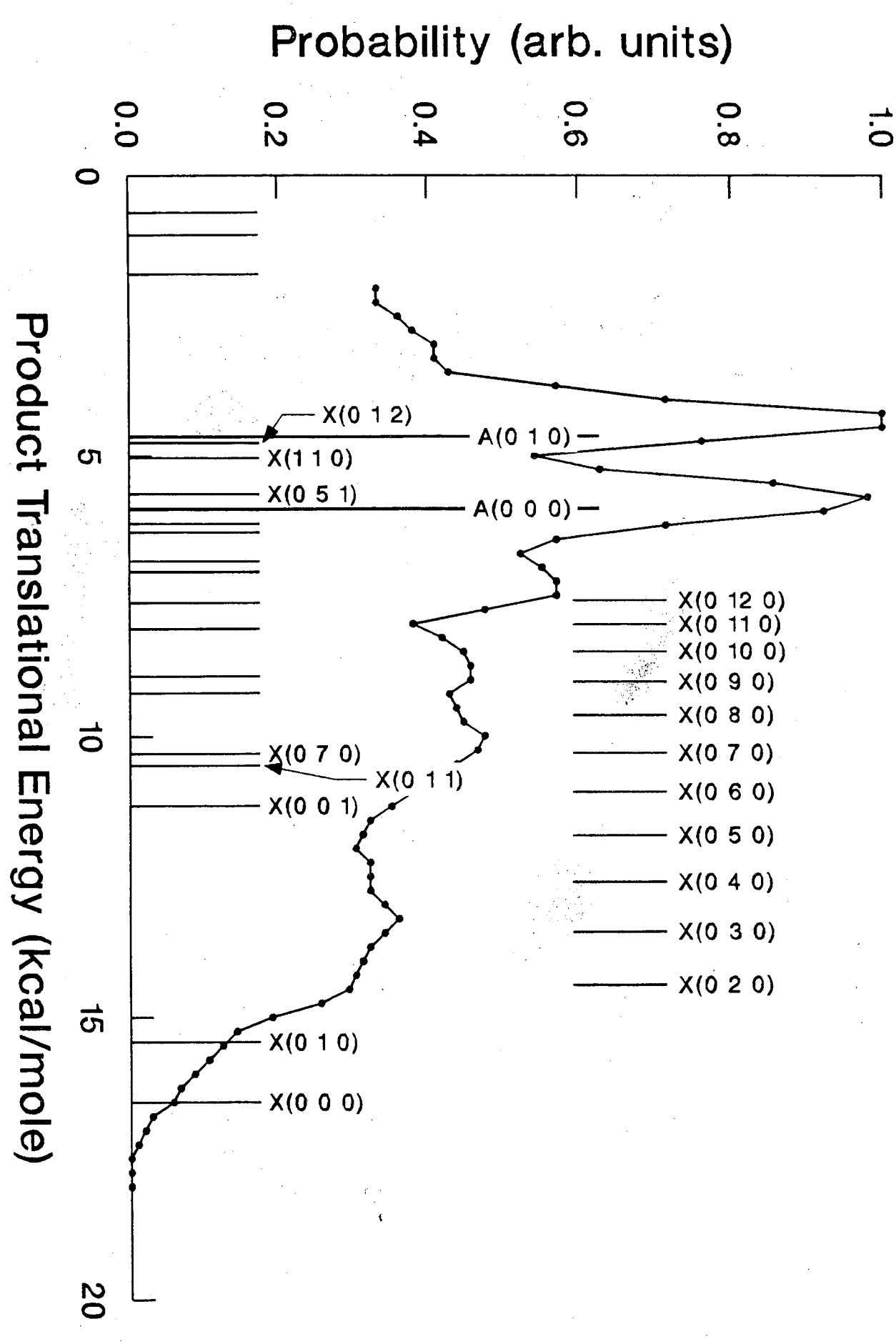
Probability (arb. units)
0.0
0.2
0.4
0.6
0.8
1.0
Product Translational Energy (kcal/mole)
0
5
10
15
20
X(0 1 2)
A(0 1 0)
X(1 1 0)
X(0 5 1)
A(0 0 0)
X(0 12 0)
X(0 11 0)
X(0 10 0)
X(0 9 0)
X(0 8 0)
X(0 7 0)
X(0 6 0)
X(0 5 0)
X(0 4 0)
X(0 3 0)
X(0 2 0)
X(0 7 0)
X(0 1 1)
X(0 0 1)
X(0 1 0)
X(0 0 0)

Figure 11

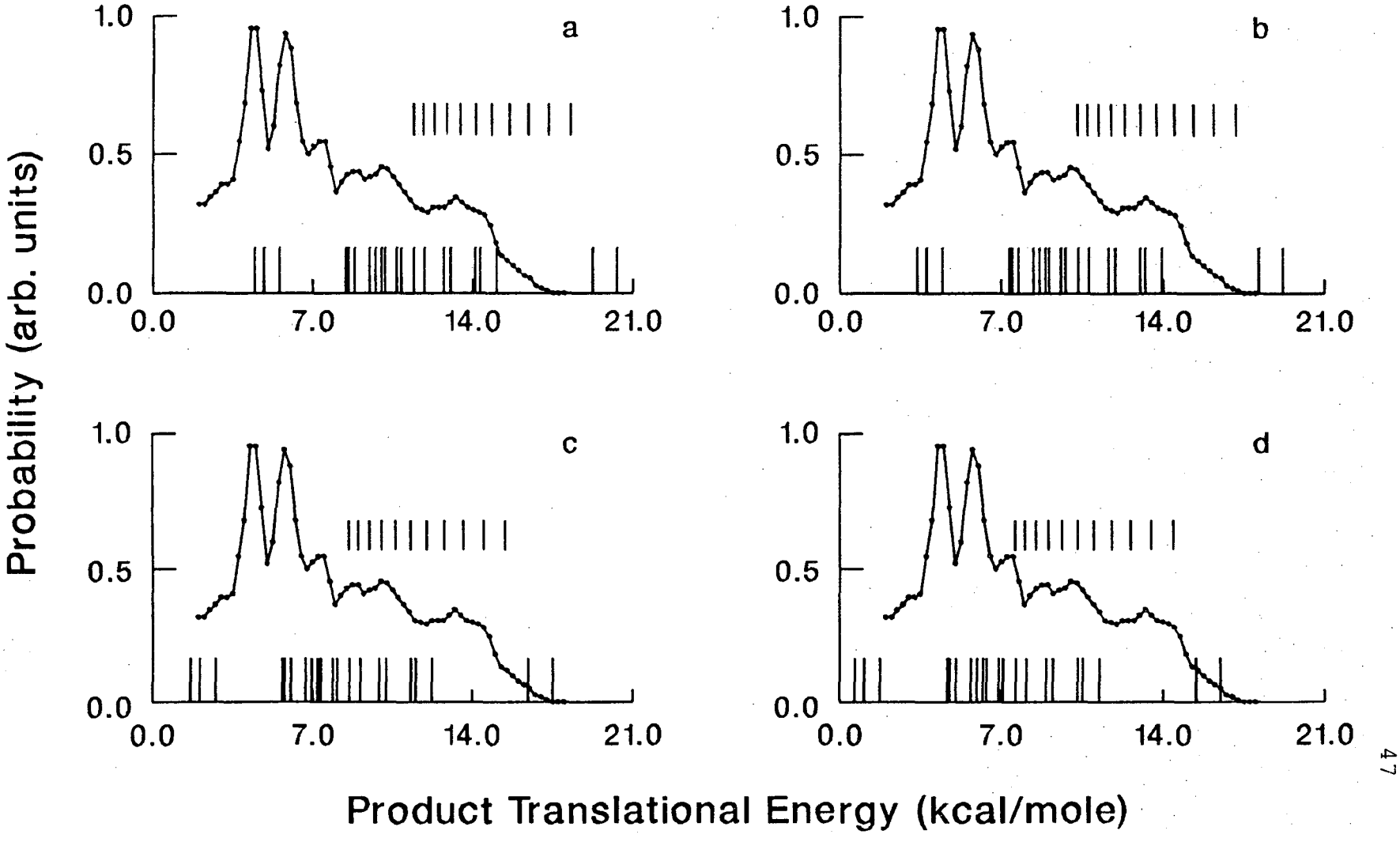
Probability (arb. units)
1.0
0.5
0.0
a
b
c
d
0.0
7.0
14.0
21.0
Product Translational Energy (kcal/mole)

Figure 12

LAWRENCE BERKELEY LABORATORY
UNIVERSITY OF CALIFORNIA
INFORMATION RESOURCES DEPARTMENT
BERKELEY, CALIFORNIA 94720